Fuel 108 (2013) 833–839

Contents lists available at SciVerse ScienceDirect

Fuel

journal homepage: www.elsevier.com/locate/fuel

Alkali activated materials based on fluid catalytic cracking catalyst residue (FCC): Influence of SiO_2/Na_2O and H_2O/FCC ratio on mechanical strength and microstructure

M.M. Tashima [a], J.L. Akasaki [b], J.L.P. Melges [b], L. Soriano [a], J. Monzó [a], J. Payá [a,*], M.V. Borrachero [a]

[a] Instituto de Ciencia y Tecnología del Hormigón, Universitat Politècnica de València, Camino de Vera s/n, Edificio 4G, 46022 Valencia, Spain
[b] UNESP – Univ Estadual Paulista, Campus de Ilha Solteira, Alameda Bahia, 550, CEP: 15385-000, Ilha Solteira SP, Brazil

HIGHLIGHTS

- An alternative alumino-silicate material for alkali activation is tested: spent FCC.
- Alkali activation of FCC has been achieved using different Na_2O/SiO_2 molar ratio and H_2O/FCC mass ratio.
- The optimisation of alkaline solution parameters was carried out.
- Alkali activated mortars are mechanically stable (some of the prepared mixtures yielded more than 60 MPa).

ARTICLE INFO

Article history:
Received 18 January 2013
Received in revised form 19 February 2013
Accepted 20 February 2013
Available online 13 March 2013

Keywords:
Spent FCC
Waste
Alkali activated material
Mechanical properties

ABSTRACT

Reuse of industrial and agricultural wastes as supplementary cementitious materials (SCMs) in concrete and mortar productions contribute to sustainable development. In this context, fluid catalytic cracking catalyst residue (spent FCC), a byproduct from the petroleum industry and petrol refineries, have been studied as SCM in blended Portland cement in the last years. Nevertheless, another environmental friendly alternative has been conducted in order to produce alternative binders with low CO_2 emissions. The use of aluminosilicate materials in the production of alkali-activated materials (AAMs) is an ongoing research topic which can present low CO_2 emissions associated. Hence, this paper studies some variables that can influence the production of AAM based on spent FCC. Specifically, the influence of SiO_2/Na_2O molar ratio and the H_2O/spent FCC mass ratio on the mechanical strength and microstructure are assessed.

Some instrumental techniques, such as SEM, XRD, pH and electrical conductivity measurements, and MIP are performed in order to assess the microstructure of formed alkali-activated binder. Alkali activated mortars with compressive strength up to 80 MPa can be formed after curing for 3 days at 65 °C. The research demonstrates the potential of spent FCC to produce alkali-activated cements and the importance of SiO_2/Na_2O molar ratio and the H_2O/spent FCC mass ratio in optimising properties and microstructure.

1. Introduction

According to the literature, Portland cement production is responsible at least 5–8% of global CO_2 emissions [1]. Concerning to the environmental problems caused by the cement industry, several studies have been reported in order to reduce the greenhouse gas emission. The reuse of waste materials generated from industrial or agricultural activities has been successfully used in the production of blended Portland cement in the last decades. The partial substitution of Portland cement by supplementary cementitious materials can reduce from 886 kg to 660 kg the CO_2 emissions associated to the production of 1 ton of Portland cement [2].

Another possibility for reducing the CO_2 emissions associated to the Portland cement industry is the production of alternative binders with low CO_2 emissions. Among these alternative materials, alkali-activated materials (AAMs), as well as reducing CO_2 emissions up to 80%, can present similar or even higher compressive strength, acid resistance, fire resistance and low shrinkage, when compared to Portland cement [3]. Alkali-activated binders

* Corresponding author. Tel.: +34 96 3877564.
E-mail addresses: maumitta@hotmail.com (M.M. Tashima), akasaki@dec.feis.unesp.br (J.L. Akasaki), jlmelges@dec.feis.unesp.br (J.L.P. Melges), lousomar@upvnet.upv.es (L. Soriano), jmmonzo@cst.upv.es (J. Monzó), jjpaya@cst.upv.es (J. Payá), vborrachero@cst.upv.es (M.V. Borrachero).

0016-2361/$ - see front matter © 2013 Elsevier Ltd. All rights reserved.
http://dx.doi.org/10.1016/j.fuel.2013.02.052

are formed by a network of SiO_4 and AlO_4 tetrahedra linked by sharing oxygen atoms. Positive ions such as Na^+, K^+, Mg^{2+} or Ca^{2+} must be present in the framework cavities to balance the charge deficiency of Al^{3+} as compared to Si^{4+}. It forms a three dimensional network of Si^{4+} and Al^{3+} in 4-fold coordination with oxygen [3,4].

The formed alkali-activated binder has either amorphous or nano-crystalline microstructure, depending basically on the amount of aluminosilicate solid material and on its nature (mineralogy of raw materials) as well as on the alkalinity of activating solution and on the curing conditions [5–8]. As can be observed in the literature, most of papers are related to the use of blast furnace slag [9–11], fly ash [12,13] and metakaolin [14,15] as an aluminosilicate material in the production of alkali-activated materials. Nevertheless, other aluminosilicate materials have also been studied for this propose such as, tungsten waste mine [16], glass fibre waste [17], air pollution control APC residues [18,19], hydrated-carbonated cement [20].

In this paper the use of fluid catalytic cracking catalyst residue (spent FCC) is assessed as an aluminosilicate material for the production of alkali-activated binders. Spent FCC is an inorganic material obtained as a byproduct from petroleum industry and petrol refineries. A correct destination for this byproduct can contribute to reducing environmental problems and, so on, it can diminish the landfill areas.

The chemical composition of spent FCC is made up mainly of aluminium and silicon oxides (aluminosilicate material), containing some impurities such as lanthanide oxides. Studies performed by Payá et al. [21] shows that independently from the origin of spent FCC, this byproduct presents a homogeneous bulk. This fact may contribute to the indiscriminate use of spent FCC in building construction.

Respect to the use of spent FCC in the production of blended concrete and mortars, a lot of studies have been reported in the literature about its pozzolanic reactivity, mechanical properties and durability aspects [22–24]. Payá et al. [22] reported a systematic study about pozzolanic activity of spent FCC in lime pastes, comparing the results to metakaolin which is considered a high reactive pozzolanic material. The authors observed that both pozzolans exhibited very high percentages of fixed lime even for early curing age and, the mainly hydrated products formed are CSH, CASH and CAH.

When spent FCC is used in blended mortars, the optimum replacement percentage is in the range 10–20%, yielding a compressive strength gain about 10 MPa, comparing to the control mortar [23]. Durability aspects are extensively assessed by Zornoza et al. [24,25] such as chloride-induced corrosion steel, accelerated carbonation, chloride ingress. In terms of durability, spent FCC blended Portland cement presented good behaviour.

The first study related to the use of spent FCC as aluminosilicate material in the production of alkali-activated materials has been recently reported by Tashima et al. [26]. In that study, authors concluded that, in general terms, an increase in the SiO_2/Na_2O molar ratio in the range 0–1.46 for a fixed Na^+ concentration (10 mol kg^{-1}), promotes an increment on the mechanical strength of mortars, yielding 8–68 MPa after 3 curing days at 65 °C. It was also observed the existence of an optimum SiO_2/Na_2O molar ratio (1.17) for a fixed Na^+ concentration. Hence, the aim of this paper is to assess the effect of SiO_2/Na_2O molar ratio, but now, varying both $\%Na_2O$ and $\%SiO_2$ percentages. Mechanical and microstructural properties of alkali-activated binders based on spent FCC are assessed. A new experimental technique based on pH and electrical conductivity measurements is performed in order to assess the progress of alkali activation reaction. Besides, the influence of H_2O/spent FCC mass ratio on the mechanical strength of mortars and on the porosity is also evaluated.

2. Experimental

2.1. Materials

Spent FCC used in this study was supplied by BP Oil – Spain. The chemical composition of spent FCC, determined by X-ray fluorescence (XRF), is summarised in Table 1. Fig. 1 shows a scanning electron micrograph of spent FCC particles. The natural spent FCC shows spherical particles with a wide particle size range (see Fig. 1a). In this study, spent FCC was previously dry milled during 20 min (see Fig. 1b) in order to obtain particle diameter about 17 μm [27].

Sodium hydroxide pellets (98% purity) supplied by Panreac S.A., and sodium silicate solution (waterglass, 28% SiO_2; 8% Na_2O; 64% H_2O) from Merck, were used in the preparation of activating solutions. For mortar specimen preparation, siliceous sand with a fineness modulus of 4.1 and a specific gravity of 2680 kg/m^3 was used.

2.2. Tests performed on alkali activated binders

Mechanical strength tests were performed by using a universal test machine following the procedures described on UNE-EN 196-1. The compressive strength value was the average of six specimens. Mercury Intrusion Porosimetry (MIP, Micromeritics Instrument Corporation) was used to evaluate the pore size distribution in alkali-activated spent FCC (AA-FCC) mortars. The intrusion pressure applied was between 14 kPa and 227.4 MPa, equivalent to pores with diameters ranging from 91.26 μm to 5.5 nm.

Microstructural characterizations of AA-FCC are assessed by several instrumental techniques. X-ray diffraction (XRD, Philips PW1710 with Cu Kα radiation in 2θ range 5–55°) was used to characterise the crystalline and semi-crystalline phases in AA-FCC paste samples. Scanning electron microscopy (SEM, JEOL JSM-6300) was used to examine the microstructure of fracture surfaces. Thermogravimetric analysis (TGA, 850 Mettler Toledo thermo-balance) used 100 μL aluminium crucibles and a nitrogen atmosphere. Samples were heated from 35 to 600 °C at 10 °C/min to give a total mass loss (%) associated with the dehydration/dehydroxilation of alkali-activated binder based on spent FCC.

To assess the formation of alkali-activated binders based on spent FCC, a new experimental technique is proposed. The analysis was performed using 1 g of crushed alkali-activated paste and 10 mL of deionized water. A continuous stirring was conducted during 10 min to allow dissolution of free ions in the suspension. After that, electrical conductivity and pH measurements of suspension were performed: a Crison microCM2201 conductimeter and a Crison micropH2001 pH-meter were used (alkali-resistant pH-electrode Crison 5204). The analysis was performed at different curing ages in order to assess the combination of sodium, hydroxyl and silicate ions in the alkali activation process: pH and electrical conductivity values in aqueous suspension should be diminished according to the alkali activation reaction progress.

2.3. Synthesis of alkali activated binders

In previous study related to the production of alkali-activated binders based on spent FCC [26], it was noted that for a fixed Na^+ concentration (10 mol kg^{-1}), the increment in the SiO_2/Na_2O molar ratio improves significantly the mechanical strength of

Table 1
Chemical composition of spent FCC (wt%).

Oxide (%)	SiO_2	$A1_2O_3$	Fe_2O_3	MgO	CaO	Na_2O	K_2O	Other
Spent FCC	46.04	47.47	0.58	0.17	0.11	0.30	0.02	5.31

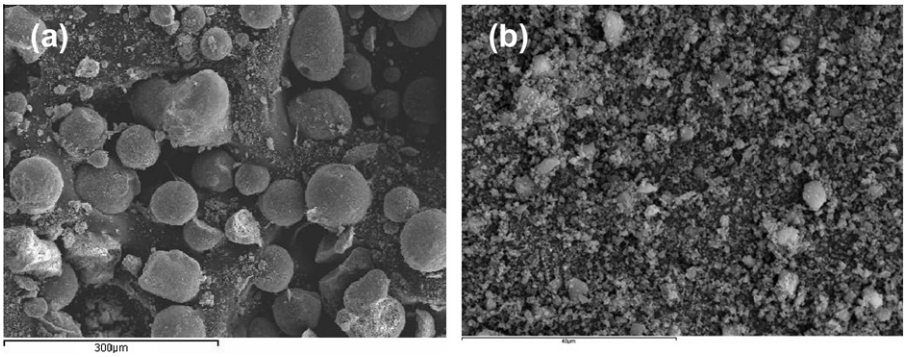

Fig. 1. SEM images of spent FCC particles: (a) before milling; (b) after milling.

alkali-activated mortars based on spent FCC. Hence, in the first part of this paper the influence of Na^+ concentration for a fixed $\%SiO_2$ (21.0% of SiO_2) is assessed. The $\%SiO_2$ was fixed according to the obtained results reached in previous work [26] and the $\%Na_2O$ was in the range 9.3–27.9% (5.0–15.0 mol kg^{-1}). All AA-FCC mortars were cured during 3 days at 65 °C with relative humidity about 95%. Table 2 summarises the activating solutions used in the production of these mortars. For all the cases, $\%Na_2O$ and $\%SiO_2$ were calculated respect to the mass of spent FCC.

Activating solutions were prepared at least 30 min prior their use to allow the solution to cooling down at room temperature. AA-FCC mortar samples were prepared by mixing spent FCC with activating solution for 4 min. Siliceous sand was then added to the paste (sand/FCC mass ratio of 3), and mortar was mixed for a further 3 min. The fresh mortars were cast in prismatic moulds (4 cm × 4 cm × 16 cm) and vibrated for 3 min to remove any air voids. The moulds were then sealed with a plastic film to avoid atmospheric carbonation and stored in a thermal bath at 65 °C for 4 h. Samples were then demoulded and stored under the same curing conditions during 3 days.

Based on the obtained results from the first part of this work and on previous work reported by Tashima et al. [26], it was decided to perform an experimental method to assess the effect of both $\%Na_2O$ and $\%SiO_2$. An experimental method was carried out using two factors ($\%SiO_2$ and $\%Na_2O$) and three levels for both factors (15.75, 21.0 and 26.25 for $\%SiO_2$ and, 13.95, 18.60 and 23.25 for $\%Na_2O$, respectively). Thus, nine activating solutions were used for mortars preparation in this part of work and its composition is summarised in Table 3.

As can be observed in Table 3, mixtures were named according to the $\%Na_2O$ and $\%SiO_2$ content. Therefore, three levels of $\%Na_2O$ content (represented by upper case letters) and three levels of $\%SiO_2$ content (represented by lower case letters) were studied (named low "L" or "l", intermediate "M" or "m", and High "H" or "h", respectively). For better understanding of adopted nomenclature, some examples of mix proportion are shown: mixture L-m represents a low content of $\%Na_2O$ (13.9%) and an intermediate content in $\%SiO_2$ (21.0%). Otherwise, mixture M-l represents an intermediate content of $\%Na_2O$ (18.6%) and low content in $\%SiO_2$ (15.7%). Again, all alkali-activated mortars were also cured at 65 °C during 3 days with high relative humidity (RH ~ 95%). AA-FCC pastes were also prepared in order to assess the relationship between mechanical and microstructural properties.

Finally, in the last part of this work, after assess the combined effect of $\%Na_2O$ and $\%SiO_2$, a specific study related to the influence of H_2O/spent FCC mass ratio was performed for a selected mix proportion. For this case, H_2O/spent FCC mass ratio was in the range 0.60–0.45 and SiO_2/Na_2O molar ratio was fixed in 1.17. Table 4 summarises the mix proportions for alkali activated mortars assessed in the last section.

Table 2
Activating solutions used in the study of the influence of Na^+ concentration for a fixed $\%SiO_2$.

Mixture	$\%Na_2O$	$\%SiO_2$	SiO_2/Na_2O	H_2O/Na_2O
AA-FCC 9.3	9.3	21.0	2.33	22.22
AA-FCC 13.9	13.9	21.0	1.56	14.81
AA-FCC 18.6	18.6	21.0	1.17	11.11
AA-FCC 23.25	23.25	21.0	0.93	8.89
AA-FCC 27.9	27.9	21.0	0.78	7.41

Table 3
Mix proportion of activating solutions varying both $\%Na_2O$ and $\%SiO_2$.

Mixture	$\%Na_2O$	$\%SiO_2$	SiO_2/Na_2O	H_2O/Na_2O
L-l	13.95	15.75	1.17	14.81
L-m	13.95	21.00	1.56	14.81
L-h	13.95	26.25	1.94	14.81
M-l	18.60	15.75	0.88	11.11
M-m	18.60	21.00	1.17	11.11
M-h	18.60	26.25	1.46	11.11
H-l	23.25	15.75	0.70	8.89
H-m	23.25	21.00	0.93	8.89
H-h	23.25	26.25	1.17	8.89

3. Results and discussion

3.1. Influence of Na^+ concentration for a fixed $\%SiO_2$

Fig. 2 shows the influence of $\%Na_2O$ for a fixed $\%SiO_2$ (21.0%) on the mechanical strength of AA-FCC mortars cured during 3 days at 65 °C. Alkali-activated mortar with the lowest $\%Na_2O$ presents a compressive strength about 10 MPa. The low compressive strength data obtained is related to a lack of alkalinity in the activating solution, which reduces the dissolution process of aluminosilicate materials and, consequently, the binder formation [28].

Increasing the $\%Na_2O$, an enhancement on the mechanical strength was observed, yielding a maximum strength value (68.3 MPa) for 18.6%Na_2O that represents a total Na^+ concentration of 10 mol kg^{-1}.

Table 4
Mix proportion of alkali activating solutions for different H_2O/spent FCC mass ratio.

Mixture	$\%Na_2O$	$\%SiO_2$	SiO_2/Na_2O	H_2O/Na_2O
M-m-0.60	18.60	21.00	1.17	11.11
M-m-0.55	17.05	19.25	1.17	11.11
M-m-0.50	15.5	17.5	1.17	11.11
M-m-0.45	13.95	15.75	1.17	11.11

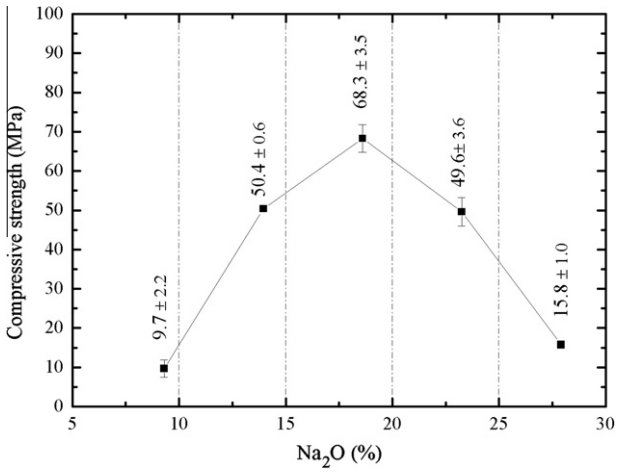

Fig. 2. Influence of $\%Na_2O$ for a fixed $\%SiO_2$ (21.0%) on the mechanical strength of AA-FCC mortars cured during 3 days at 65 °C.

Somna et al. [29] also observed the existence of an optimum Na_2O concentration ranging from 9 to 14 M for alkali-activated fly ash systems.

For the activating solutions with 23.25%Na_2O, the compressive strength started to decline due to the fact that for high OH^- concentration the dissolution process is accelerated, but, on the other hand, polycondensation process is restricted [30]. Besides it, an excess of OH^- ions causes a rapid precipitation of aluminosilicate gels (zeolitic precursors), yielding low mechanical strength binders [31].

Hence, the existence of an optimum $\%Na_2O$ value is observed for a fixed $\%SiO_2$, obtaining alkali-activated mortars about 68 MPa after 3 curing days at 65 °C. Several papers [32,33] also reported the existence of an optimum alkali concentration for alkali activated materials.

3.2. Influence of both $\%Na_2O$ and $\%SiO_2$

3.2.1. Mechanical strength

Compressive strengths of alkali-activated mortars based on spent FCC prepared using different $\%Na_2O$ and $\%SiO_2$ proportions are given in Table 5. Compressive strengths vary from 26 to 68 MPa with higher compressive strength obtained for mixture M-m, it means, for 18.6% of Na_2O and 21.0% of SiO_2. This mixture presents a SiO_2/Na_2O molar ratio of 1.17 and a H_2O/Na_2O molar ratio of 11.11.

Fig. 3 shows a non-linear fitting surface of compressive strength values for alkali-activated mortars based on spent FCC. It can be observed that there is a large region where AA-FCC mortars have compressive strength values higher than 60 MPa (from 16% to 22%SiO_2 and from 14% to 20%Na_2O), indicating that in this range of composition for the activating solution, there is no excessive influence of SiO_2/Na_2O molar ratio. Nevertheless, it can be noted a strong dependence between compressive strength values and SiO_2/Na_2O molar ratio for the outer region.

Table 5
Compressive strength values for alkali activated mortars using different $\%Na_2O$ and $\%SiO_2$ concentrations.

Mixture	$\%Na_2O$	$\%SiO_2$	R_c (MPa)
L-l	13.95	15.75	59.7 ± 3.2
L-m	13.95	21.00	67.5 ± 3.1
L-h	13.95	26.25	26.4 ± 1.6
M-l	18.60	15.75	58.6 ± 2.1
M-m	18.60	21.00	68.3 ± 3.5
M-h	18.60	26.25	58.9 ± 4.4
H-l	23.25	15.75	32.8 ± 2.4
H-m	23.25	21.00	49.6 ± 3.6
H-h	23.25	26.25	53.7 ± 1.6

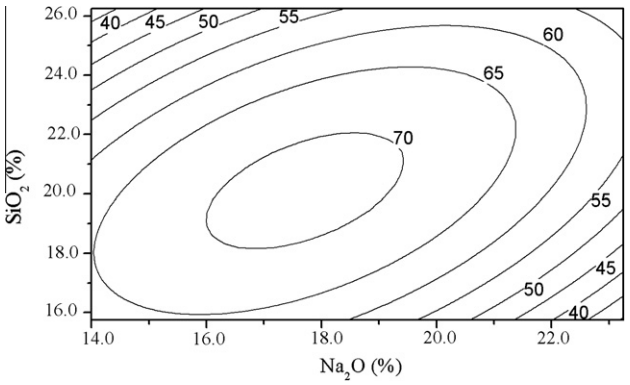

Fig. 3. Non-linear fitting surface of compressive strength for alkali activated mortars based on spent FCC.

From the non-linear fitting surface equation, it can be established the optimised value of compressive strength for alkali-activated mortars based on spent FCC. Theoretically, the maximum value of compressive strength, calculated by the derivative point of non-linear fitting curve equation, for alkali-activated mortars is 71 MPa.

Comparing the maximum value obtained experimentally (mixture M-m) with the theoretical calculated value, it can be observed that the difference in compressive strength is negligible. Hence, in this case, mixture M-m (18.6% of Na_2O and 21.0% of SiO_2) is considered the optimised mixture for the studied conditions. The specific study related to the effect of H_2O/spent FCC mass ratio on the mechanical strength and porosity of AA-FCC mortars is going to be performed with the optimised mixture, it means, the mixture M-m.

3.2.2. Microstructural studies

The mineralogy of formed products in the alkali activation process of spent FCC was assessed by means of X-ray diffractions. Fig. 4 shows the XRD patterns for selected alkali-activated pastes (mixtures M-l, M-m and M-h) cured after 3 days at 65 °C. XRD pattern for spent FCC sample is also depicted. The main crystalline component identified in spent FCC sample is acid-faujasite (in sodium form $Na_2Al_2Si_4O_{12}{\cdot}8H_2O$, PDFcard# 391380). For

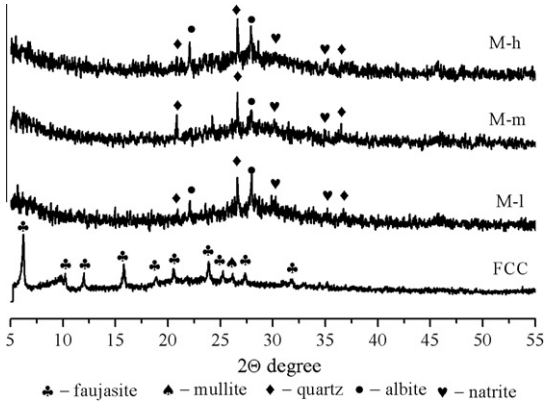

Fig. 4. X-ray diffractograms for spent FCC sample and selected alkali activated mixtures: M-l, M-m and M-h.

alkali-activated pastes, it is observed a baseline deviation in the range 23–32°, suggesting an important presence of amorphous phase. Comparing to the baseline deviation of FCC sample (2Θ = 17–30°), there was a shift to 2Θ higher values due to the geopolymerisation reaction that forms new amorphous gel. Similar results were also reported by Provis et al. [34].

Respect to the crystalline phases, it can be noted the presence of quartz (SiO_2, PDFcard# 331161), albite ($NaAlSi_3O_8$, PDFcard# 090466) and natrite (Na_2CO_3, PDFcard# 370451) in the microstructure of alkali-activated pastes. Quartz and albite were present in the spent FCC sample as minor component and, due to the dissolution process of faujasite compound, the presence of these components are evidenced in alkali-activated pastes. Sodium carbonate is formed in alkali activated pastes due to carbonation or the presence of impurities in the sample (alkaline reagents).

Fig. 5 shows micrographs of selected alkali activated pastes based on spent FCC (mixtures L-l, M-m and H-l). The L-l paste shown in Fig. 5a and b has an amorphous microstructure with a significant amount of partially and/or unreacted spent FCC particles. The M-m paste shown in Fig. 5c–e has a dense-compact and amorphous microstructure. However, some particles of partially reacted spent FCC are also observed. Similar microstructural feature have been observed in other alkali-activated systems [17,19]. Fig. 5f shows a general view of the H-l paste. It is not observed the presence of unreacted spent FCC particles in matrix. According to the literature a high alkaline solution contributes to the dissolution process, but hinders the polymerisation reaction [30]. This statement was verified in the compressive strength tests, obtaining matrix with not so good performance due to the precipitation of hydrated products at early ages.

The progress of alkali-activated reaction was monitored by means of pH and electrical conductivity measurements in an aqueous suspension only for mixture M-m. A decrease on these values indicates the progress of alkali activation reaction.

The initial pH for the sample M-m (5 min of mixing at room temperature) was 13.01: obviously this in not the pH of the water solution in the pores of AA-FCC paste, because this is the pH of a diluted solution after mixing 1 part of alkali-activated paste and 10 parts of deionized water. In the same conditions, the electrical conductivity was 23.1 mS/cm. This electrical conductivity value is considered as the contribution of all ions that can move under an electric field in an aqueous medium.

Fig. 6 shows the evolution of pH and electrical conductivity measurements with curing time for pastes cured at 65 °C. It is noticeable that both parameters diminish with curing time progress, and this reduction is very important in the first 2 h of reaction.

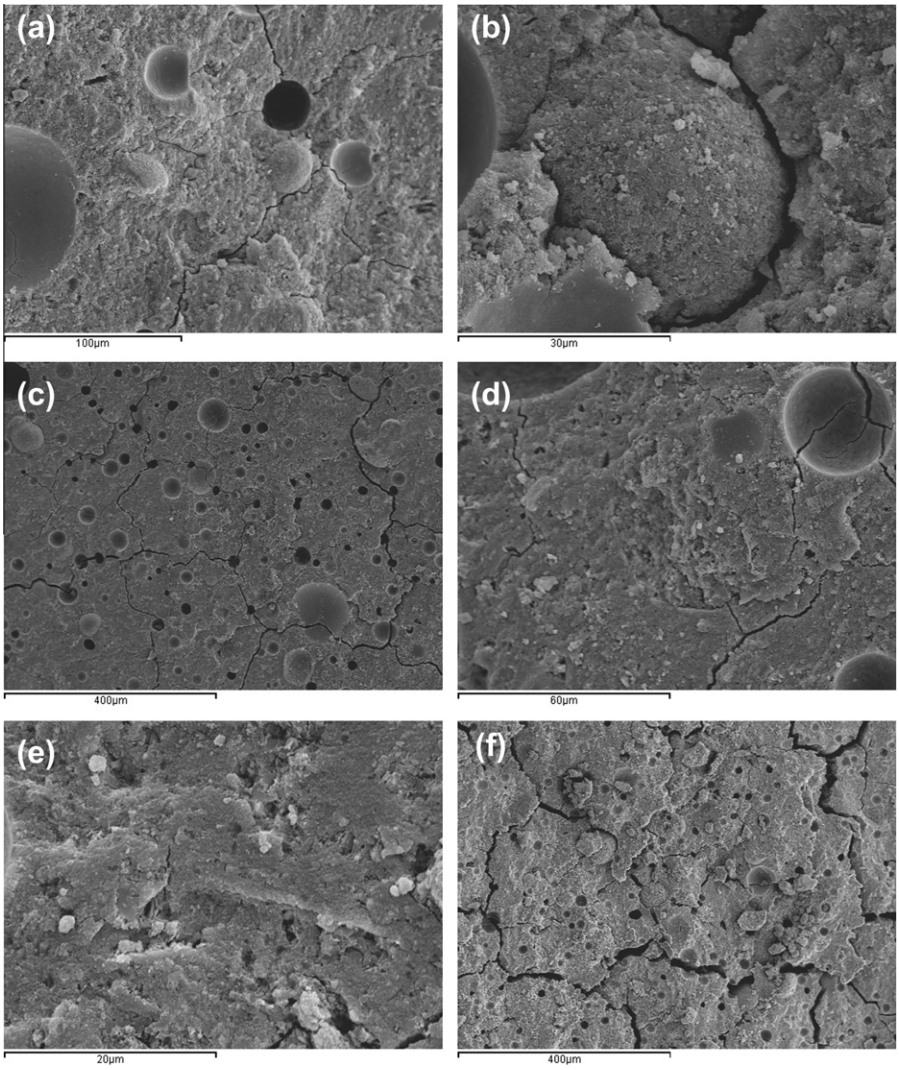

Fig. 5. SEM micrographs of geopolymeric pastes: L-l mixture (micrographs a and b); M-m mixture (micrographs c–e); H-l mixture (micrograph f).

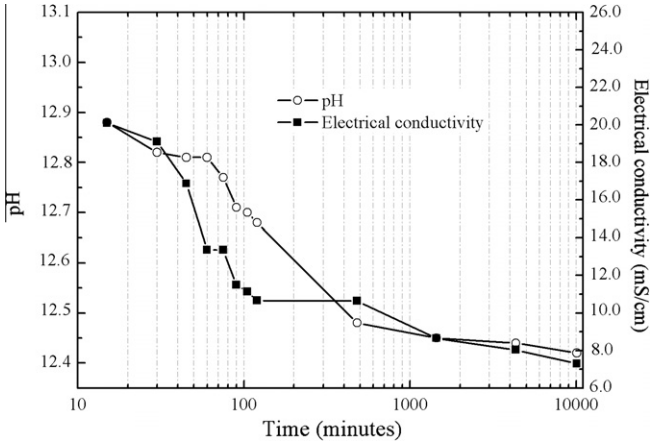

Fig. 6. Electrical conductivity and pH evolution for M-m mixture.

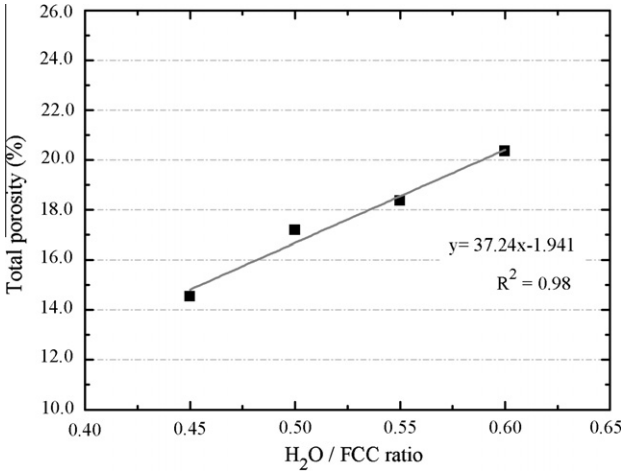

Fig. 7. Influence of H_2O/FCC ratio on total porosity (%) of alkali activated mortars.

Table 6
Compressive strength of alkali-activated mortars prepared for studying the influence of H_2O/FCC mass ratio.

Mixture	%Na_2O	%SiO_2	R_c (MPa)
M-m-0.60	18.60	21.00	68.3 ± 3.5
M-m-0.55	17.05	19.25	71.4 ± 5.9
M-m-0.50	15.5	17.5	79.1 ± 1.6
M-m-0.45	13.95	15.75	83.6 ± 3.6

After 120 min, the pH value was reduced to 12.68, which means that the OH^- concentration was diminished in 52%: this behaviour suggests that the cleavage of Si–O–Si and Si–O–Al bonds by the action of OH^- anions is a relevant step for the first hours. Associated to the pH reduction, there is a parallel decrease of electrical conductivity: 10.6 mS/cm was obtained after 120 min, which corresponds to a reduction in electrical conductivity of 54%. It is noteworthy that both reductions are similar.

After 7 days of reaction, the electrical conductivity is about 7.5 mS/cm and the pH value is 12.42. Similar values were reached after only 1 day of reaction, indicating that alkali activation reaction of spent FCC occurs in the first 24 h and, after that, the small variations in the electrical conductivity and pH values represents the rearranging of the microstructure of AA-FCC paste.

3.3. Influence of H_2O/FCC mass ratio

3.3.1. Mechanical strength tests

Table 6 summarises the mechanical strength of alkali activated mortars with different H_2O/FCC mass ratio. For all alkali activating solution, the SiO_2/Na_2O molar ratio was fixed in 1.17 and the H_2O/FCC was in the range 0.60–0.45.

According to the obtained results (see Table 6), compressive strength values obtained for different H_2O/FCC mass ratio present a linear dependence, achieving values around 80 MPa for the mixture M-m 0.45. The results confirm the importance of H_2O/FCC mass ratio on mechanical strength of alkali-activated binders.

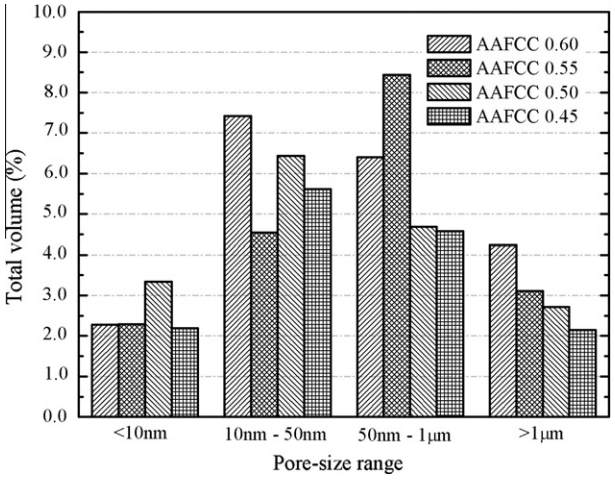

Fig. 8. Pore size distributions for M-m mortars.

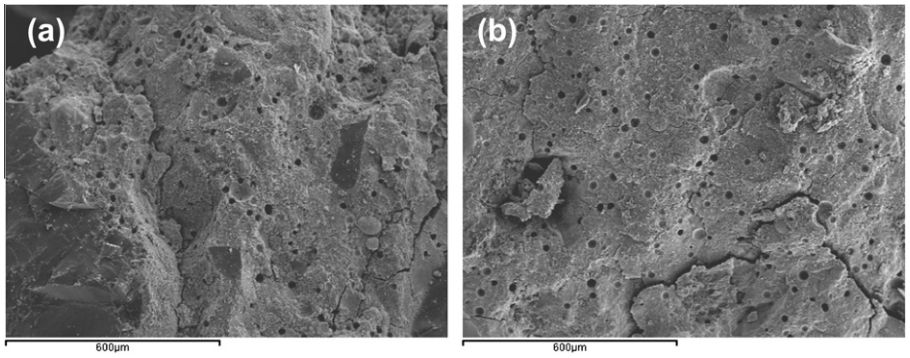

Fig. 9. SEM micrographs of alkali-activated mortars with different H_2O/FCC ratio: (a) 0.45; (b) 0.60.

3.3.2. Microstructural properties

The total porosity of alkali-activated mortars was measured by means of MIP test. A direct relationship between total porosity and H_2O/FCC mass ratio can be established. The total porosity values are in the range 14.5–20.5% in volume, depending on the H_2O/FCC ratio (see Fig. 7).

The pore size distributions for M-m with different H_2O/FCC ratio are shown in Fig. 8. It can be noted that the volume of gel pores (diameter less than 10 nm) was very low, whereas the volumes of capillary pores are very important. There is no refinement of pores size when the amount of water was diminished. However, a clear trend was observed for large pores with diameter greater than 1 μm. The volume of this type of pores was reduced when diminishing the H_2O/FCC ratio. This behaviour suggests that for alkali-activated mortars based on FCC the main factor related to compressive strength is the total porosity.

Two selected mortars (M-m 0.45 and M-m 0.60) were studied by SEM. Selected micrographs are shown in Fig. 9. In both mortars, a dense and compact microstructure is observed with the presence of air voids (20–100 μm). No microstructural differences can be observed for the selected mortars.

4. Conclusions

In this paper, the influence of alkali activating solution on properties of alkali-activated materials based on spent FCC is reported, and it is concluded that the SiO_2/Na_2O molar ratio and H_2O/FCC mass ratio have a key role on the mechanical and microstructural properties of the pastes and mortar samples formed. All AA-FCC mortars with H_2O/FCC of 0.6 had a compressive strength in the range of 26–68 MPa when cured at 65 °C for 3 days in high humidity environment. And an optimised alkaline activating solution was achieved for 18.6% of Na_2O and 21.0% of SiO_2. The new experimental technique proposed, pH and electrical conductivity measurements in an aqueous suspension prepared from ground AA paste has allowed the monitoring of the progress of alkali activation.

A reduction in the H2O/FCC mass ratio is related to an increment in the compressive strength of AA-FCC and a reduction in the total porosity of these samples. Compressive strength of 80 MPa was achieved for mortars with H_2O/FCC mass ratio of 0.4 with a total porosity of 14.5% in volume.

Acknowledgments

Authors would like to thank to the Ministerio de Ciencia e Innovación (MICINN) of the Spanish Government (BIA2011-26947) and to FEDER for funding, and also to the PROPG – UNESP "Universidade Estadual Paulista Julio de Mesquita Filho", Brazil.

References

[1] Shi C, Fernández-Jiménez A, Palomo A. New cements for the 21st century: the pursuit of an alternative to Portland cement. Cem Concr Res 2011;41:750–63.
[2] WSCSD – World Business Council for Sustainable Development. Cement industry energy and CO_2 performance – Getting numbers right; 2009.
[3] Alcaide JS, Alcocel EG, Puertas F, Lapuente R, Garcés P. Carbon fibre-reinforced, alkali-activated slag mortars. Mater Construcc 2007;57:33–48.
[4] Fernández-Jiménez A, Palomo A. Composition and microstructure of alkali activated fly ash binder: effect of the activator. Cem Concr Res 2005;35:1984–92.
[5] Criado M, Fernández-Jiménez A, Palomo A. Alkali activation of fly ash. Part III: Effect of curing conditions on reaction and its graphical description. Fuel 2010;89:3185–92.
[6] Rahier H, Mele B, Biesemans M, Wastiels J, Wu X. Low-temperature synthesized aluminosilicate glasses. J Mater Sci 1996;31:71–9.
[7] Phair JW, van Deventer JSJ. Effect of the silicate activator pH on the microstructural characteristics of waste-based geopolymers. Int J Miner Process 2002;66:121–43.
[8] Tashima MM, Soriano L, Borrachero MV, Monzó J, Payá J. Effect of curing time on the microstructure and mechanical strength development of alkali activated binders based on Vitreous Calcium Aluminosilicate (VCAS). Bull Mater Sci, in press. http://www.ias.ac.in/matersci/
[9] Fernández-Jiménez A, Palomo JG, Puertas F. Alkali-activated slag mortars: mechanical strength behaviour. Cem Concr Res 1999;29:1313–21.
[10] Shi C, Krivenko P, Roy D. Alkali-activated cements and concretes. 1st ed. New York: Taylor & Francis; 2006.
[11] Bernal SA, Gutiérrez RM, Pedraza AL, Provis JL, Rodriguez ED, Delvasto S. Effect of binder content on the performance of alkali-activated slag concretes. Cem Concr Res 2011;41:1–8.
[12] Fernández-Jiménez A, Palomo A, Criado M. Microstructure development of alkali-activated fly ash cement: a descriptive model. Cem Concr Res 2005;35:1204–9.
[13] Bakharev T. Geopolymeric materials prepared using class F fly ash and elevated temperature curing. Cem Concr Res 2005;35:1224–32.
[14] Buchwald A, Hilbig H, Kaps C. Alkali-activated metakaolin-slag blends – performance and structure in dependence of their composition. J Mater Sci 2007;42:3024–32.
[15] Muñiz-Villareal MS, Reyes-Araiza JL, Sampieri-Bulbarela S, Gasca-Tirado JR, Manzano-Ramírez A, Rubio-Ávalos JC, et al. The effect of temperature on the geopolymerisation process of a metakaolin-based geopolymer. Mater Lett 2011;65:995–8.
[16] Pacheco-Torgal F, Castro-Gomes J, Jalali S. Properties of tungsten mine waste geopolymeric binder. Constr Build Mater 2008;22:1201–11.
[17] Tashima MM, Soriano L, Borrachero MV, Monzó J, Cheeseman CR, Payá J. Alkali activation of vitreous calcium aluminosilicate derived from glass fiber waste. J Sust Cem-Based Mater 2012;3:83–93.
[18] Kourti I, Devaraj AR, Guerrero Bustos A, Deegan D, Boccaccini AR, Cheeseman CR. Geopolymers prepared from DC plasma treated air pollution control (APC) residues glass: properties and characterisation of binder phase. J Hazard Mater 2011;196:86–92.
[19] Kourti I, Rani DA, Deegan D, Boccaccini AR, Cheeseman CR. Production of geopolymers using glass from DC plasma treatment of air pollution control (APC) residues. J Hazard Mater 2010;176:704–9.
[20] Payá J, Borrachero MV, Monzó J, Soriano L, Tashima MM. A new geopolymeric binder from hydrated-carbonated cement. Mater Lett 2012;74:223–5.
[21] Payá J, Borrachero MV, Monzó J, Soriano L. Estudio del comportamiento de diversos residuos de catalizadores de craqueo catalítico (FCC) en cement Portland. Mater Constr 2009;59:37–52.
[22] Payá J, Monzó J, Borrachero MV, Velázquez S. Evaluation of the pozzolanic activity of fluid catalytic cracking catalyst residue (FC3R). Thermogramivetric analysis studies on FC3R-Portland cement pastes. Cem Concr Res 2003;33:603–9.
[23] Payá J, Borrachero MV. Physical, chemical and mechanical properties of fluid catalytic cracking catalyst residue (FC3R) blended cements. Cem Concr Res 2001;31:57–61.
[24] Zornoza E, Garcés P, Monzó J, Borrachero MV, Payá J. Accelerated carbonation of cement pastes partially substituted with fluid catalytic cracking catalyst residue (FC3R). Cem Concr Comput 2009;31:134–8.
[25] Zornoza E, Payá J, Garcés P. Chloride-induced corrosion of steel embedded in mortars containing fly ash and spent cracking catalyst. Corros Sci 2008;50:1567–75.
[26] Tashima MM, Akasaki JL, Castaldelli VN, Soriano L, Monzó J, Payá J, et al. New geopolymeric binder based on fluid catalytic cracking catalyst residue (FCC). Mater Lett 2012;80:50–2.
[27] Payá J, Monzó J, Borrachero MV. Fluid catalytic cracking catalyst residue (FC3R): an excellent mineral by-product for improving early-strength development of cement mixtures. Cem Concr Res 1999;29:1773–9.
[28] Chindaprasirt P, Jaturapitakkul C, Chalee W, Rattanasak U. Comparative study on the characteristics of fly ash and bottom ash geopolymers. Waste Manage 2009;29:539–43.
[29] Somna K, Jaturapitakkul C, Kajitvichyanukul P, Chindaprasirt P. NaOH-activated ground fly ash geopolymer cured at ambient temperature. Fuel 2011;90:2118–24.
[30] Zuhua Z, Xiao Y, Huajun Z, Yue C. Role of water in the synthesis of calcined kaolin based geopolymer. Appl Clay Sci 2009;43:218–23.
[31] Lee WKW, van Deventer JSJ. Structural reorganization of class F fly ash in alkaline silicate solutions. Colloids Surf A 2002;211:49–66.
[32] Lampris C, Lupo R, Cheeseman CR. Geopolymerisation of silt generated from construction and demolition waste washing plants. Waste Manage 2009;29:368–73.
[33] Wu HC, Sun P. New building materials from fly ash-based lightweight inorganic polymer. Constr Build Mater 2007;21:211–7.
[34] Provis JL, Duxson P, Lukey GC, van Deventer JSJ. Statistical thermodynamic model for Si/Al ordering in amorphous aluminosilicates. Chem Mater 2005;17:2976–86.